Hindawi Publishing Corporation
International Journal of Optics
Volume 2012, Article ID 258013, 12 pages
doi:10.1155/2012/258013

Review Article

Subwavelength Plasmonic Waveguides and Plasmonic Materials

Ruoxi Yang and Zhaolin Lu

Microsystems Engineering, Kate Gleason College of Engineering, Rochester Institute of Technology, Rochester, NY 14623, USA

Correspondence should be addressed to Zhaolin Lu, zxleen@rit.edu

Received 29 March 2012; Accepted 8 June 2012

Academic Editor: Xiaoyue Huang

With the fast development of microfabrication technology and advanced computational tools, nanophotonics has been widely studied for high-speed data transmission, sensitive optical detection, manipulation of ultrasmall objects, and visualization of nanoscale patterns. As an important branch of nanophotonics, plasmonics has enabled light-matter interactions at a deep subwavelength length scale. Plasmonics, or surface plasmon based photonics, focus on how to exploit the optical property of metals with abundant free electrons and hence negative permittivity. The oscillation of free electrons, when properly driven by electromagnetic waves, would form plasmon-polaritons in the vicinity of metal surfaces and potentially result in extreme light confinement. The objective of this article is to review the progress of subwavelength or deep subwavelength plasmonic waveguides, and fabrication techniques of plasmonic materials.

1. Introduction

Plasmonics, a name coined for surface-plasmon-(SP-) related photonics, has inspired booming research interests since late 1990s. Actually, the history of surface plasmon research dates back to the investigation of surface plasmon resonance (SPR) on metallic thin films [1], or even light scattering from nanoscale metallic particles as early as 1970s [2]. Research focus has then shifted to the integration of plasmonic components into subsystems for optical communications and information exchange, when many novel plasmonic devices have been developed for communications in recent years [3]. Accordingly, plasmonic waveguides, couplers, and modulators become the core topics of the new plasmonics era. Two factors have catalyzed and contributed to this transition. Firstly, along with the advanced numerical tools backed up by computational electromagnetics, powerful computers and computing clusters have been more affordable and accessible. More importantly, with the fast development of nano- and microfabrication technology, researchers have been empowered to fabricate complex structures and manipulate wide selection of materials. In this paper, we will review the development and progress of plasmonic waveguides, especially the applications of metal-insulator-metal waveguides, and various plasmonic materials based on their application spectrum and fabrication techniques.

2. Motivation

Light has emerged as one of the most important carriers for large volume data, as well as a reliable and powerful aide for perception and manipulation of small particles. Compared to its classical form featured with bulky objects and diffraction-limited beams, in recent years the science of optics has utilized much finer elements where the light-matter interactions are strengthened inside a much smaller length scale compared to the lightwave's wavelength. Microoptics and nanophotonics, despite the miniature size of their elements of interest, have shown remarkable impact on all kinds of applications in communications, data storage, sensing, and imaging, and so forth. However, the mode size of a dielectric waveguide is still ruled by the diffraction-limit (close to λ/n, n being the guiding area's refractive index, and λ being the vacuum wavelength of the incident wave), and further shrinking the dimension of dielectric waveguides will inevitably lead to cutoff. This limitation leads to explorations of novel guiding mechanism and materials. Waveguides based on surface plasmons and metals, as found out later, can support propagation mode tightly bounded to the metallic surfaces and possibly confine the guiding wave in deep subwavelength scale. Accordingly, plasmonics has received tremendous attention for its scope of overcoming diffraction limit.

The current trend of technology evolution is marked by the demand of small and compact devices and high-volume integration of multiple modules on the same chip. As Moore's law in Microelectronics enforces more computational power in unit area, the telecommunications has harbored the fiber-to-the-home (FTTH) conception [4] which put high emphasis on reducing the size and cost of individual optical modules. This poses significant challenges for installation of next-generation optical interconnects featuring both compact integration and faster operation, which can be addressed possibly by resorting to plasmonics.

Moreover, light has been anticipated as an indispensable tool to print ultrafine patterns and to manipulate and observe miniscule items. For instance, optical lithography has been pivotal for the prosperity of semiconductor technology [5], but its ability to pace the roadmap of very-large-scale-integration (VLSI) technology has been slowed down because of the diffraction limit of most optical imaging systems. As another example, with complex systems such as DNA sequencing facility [6] designed and developed to incorporate ultrafine optical subsystems, the cost, and quality of optical consumables interfacing with small amount of biological or chemical substances have proved to be decisive. It has also been predicted that plasmonic nanofocusing can revolutionize the traditional magnetic recording by optically heating the media stack in a highly confined fashion, according to the technology called heat-assisted magnetic recording (HAMR) or thermal assisted magnetic recording (TAMR) [7]. Plasmonics, in this sense, shall play a much larger role for optical imaging and sensing subsystem development.

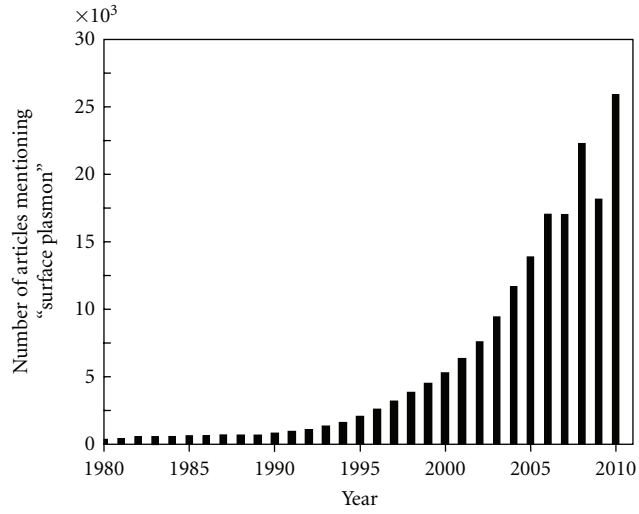

Figure 1: The growth of SP-related research in number of articles from 1980 to 2010, data acquired from Google Scholar (http://scholar.google.com/, accessed on Feb 10, 2012).

Table 1: Plasmonic frequencies and damping factors for Al, Au, Cu, and Al in NIR spectrum [12].

Material	f_p (THz)	γ_τ (THz)
Aluminum	3570	19.79
Gold	2183	6.46
Copper	1914	8.34
Silver	2180	4.353

3. Nanoplasmonic Waveguide

Research in plasmonics or other SP-related topics has gone through very fast progress in the last decade, while significant breakthroughs were reported by the end of last century (Figure 1) [8]. The study of localized SP remains active, which still finds applications from sensing, detecting, lithography, and imaging to optical storage. Since 1990, the study of plasmonic waveguides and plasmonic-enhanced (extraordinary) transmission [9] has greatly boosted the exposure of the subject. In this section, the fundamentals of plasmonics and the theory of plasmonic waveguides will be reviewed in detail.

3.1. Metal Optics with Drude Model. Metallic films are typically regarded as reflectors or cladding layers in guided-wave micro-optics for visible and near-infrared (NIR) spectrum. While metals' role in optics seems limited, the history of plasma optics is surprisingly long, although it in general lacked detailed descriptions from a guided wave perspective. Plasma optics assumes the rationality of effective dielectric constant of conduction electrons or electron gas, which determines the behavior of plasma oscillations in response to external optical driving field [10]. A plasmon is a quantized plasma oscillation, and the motion of the collective oscillation can rightly support electromagnetic (EM) waves at optical frequencies. With a frequency-dependent conductivity being prescribed, a classical Lorentz equation of motion can be used to derive the effective permittivity [11], providing the frequency independent plasma frequency $\omega_p = \sqrt{Ne^2/\varepsilon_0 m}$, while N describes the electron concentration, e the unit electric charge, ε_0 the free space permittivity, and m the electron mass.

The volume plasma has this characteristic plasma frequency ω_p, out of which the Drude model can be used to determine the dielectric constant of metals (ε_0 the free space permittivity):

$$\varepsilon_e(\omega) = \varepsilon_0 + \frac{\sigma_0}{j\omega(1 + j\omega\tau)} \approx \varepsilon_0 - \frac{\sigma_0}{\omega^2\tau} = \varepsilon_0\left(1 - \frac{\omega_p^2}{\omega^2}\right). \quad (1)$$

In this paper, we mostly consider gold and silver for applications engaging NIR and visible light. The plasma frequencies for them are well above 1000 THz, and are in general higher than the frequency of incident optical beams. The plasma frequencies given by $f_p = \omega_p/2\pi$, and the damping factors by $\gamma_\tau = 1/\tau$ for NIR spectrum of aluminium, gold, copper, and silver are shown in Table 1, adapted from [12]. The dielectric constants of these four metals are then plotted in Figure 2 by referring to [13].

By comparing the plasma frequency with the damping factor and considering the optical application regime, we conclude that external driving field from light will in general

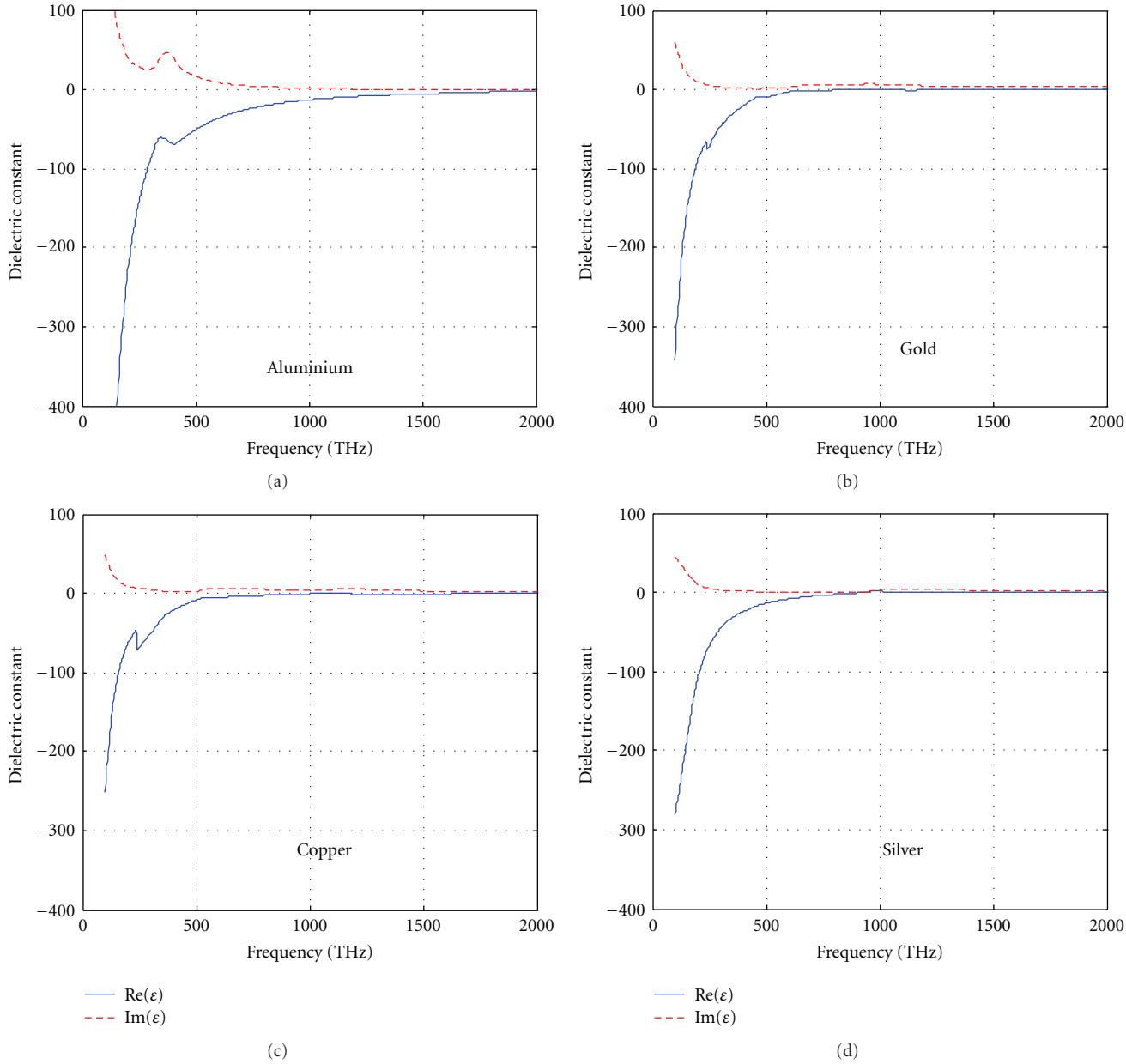

Figure 2: Dielectric constants of (a) aluminum, (b) gold, (c) copper, and (d) silver [13].

meet the prerequisite of $\omega \gg 1/\tau$ for the Drude model and the effective permittivity formalism cited above to hold. Therefore, EM waves inside plasmon environment using the effective permittivity formalism (no additional free current or conductivity term) can be characterized by the classical Helmholtz equation derived from Maxwell's equation

$$(\nabla^2 + \varepsilon_e k_0^2)\vec{E} = 0. \tag{2}$$

Note that in the Ampere's law used to derive this equation, there is no free current term. The factor of conductivity can be absorbed to the effective permittivity as below, although the following analysis will generally omit the damping factor γ_τ, assuming the form defined in (1). Therefore

$$\nabla \times \vec{H} = j\omega\tilde{\varepsilon}_e\vec{E} \approx j\omega\,\mathrm{Re}[\tilde{\varepsilon}_e]\vec{E}. \tag{3}$$

3.2. Bulk Plasma and Surface Plasmon. Considering a plane wave solution in the form of $A\exp(-j\vec{k}\cdot\vec{r})$ for (2), a dispersion relation can be obtained as

$$|k|^2 = k_0^2\varepsilon_e(\omega) = \left(\frac{\omega}{c_0}\right)^2\varepsilon_e(\omega). \tag{4}$$

Equation (4) clearly shows that a metal with positive permittivity will support plane waves in the bulk medium. In other words, if the driving frequency goes above the bulk plasma

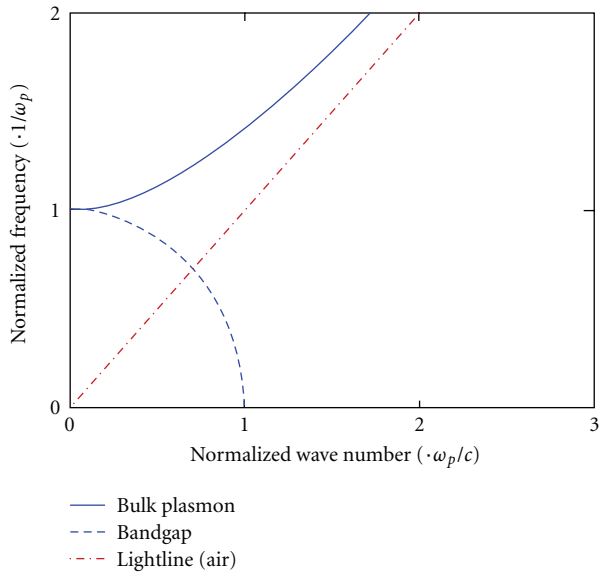

Figure 3: Dispersion relation of free electron gas (solid) compared to that of lightline of dielectric material (dash-dotted).

frequency, the plasma (or metal) becomes transparent to this external EM wave as

$$\beta = \sqrt{\varepsilon_e} k_0 = k_0 \sqrt{1 - \frac{\omega_p^2}{\omega^2}}. \quad (5)$$

This dispersion relation of free-electron gas is shown in the solid blue curve in Figure 3.

On the other hand, a negative dielectric constant is obtained when the driving frequency of the incident optical beam falls below the plasma frequency, which leads to an evanescent wave with an imaginary wave vector, as given by

$$k_{\text{eva}} = \sqrt{\varepsilon_e} k_0 = \pm j k_0 \sqrt{\frac{\omega_p^2}{\omega^2} - 1}. \quad (6)$$

This relation is shown in the dashed curve bearing a lower frequency cutoff related to plasma frequency ω_p in Figure 3. Physically, whatever direction the incident field comes from, the field will impinge into a small thickness known as skin depth, and then be fully shielded by the free electrons. The concept and the term of "skin depth" conveys an implication that only a small fraction of bulk metal could take part in the photon-material interaction, and very limited field-penetration or power-propagation could ever happen. External optical fields can only penetrate into metals for a couple of nanometers range among this spectrum, and are therefore trivial compared to the reflecting power radiated away from the metal surfaces.

The bulk plasma does not support EM waves with negative permittivity. However, it is also known that dispersion with negative permittivity has great potentials to be engineered or incorporated into complex composites for novel applications, as researchers have already done to artificially shaped structures such as photonic crystals [14] or metamaterials [15]. In this sense, the dispersion of plasmons described by the Drude model provides certainly an opportunity to manipulate electromagnetic waves and fields, as will be seen for the case of surface plasmons.

For surface plasmons, the dispersion curve will be more complex. Surface plasmon waves, which reveal the macroscopic motion of surface plasmon-polaritons (SPPs), are a coherent combination of electron gas oscillation (plasmons) and photons. For a simple case of a single metal-insulator interface in 2-dimensional (2D) view, a transverse-magnetic (TM) solution for (2) is available [1, 16]. A matched real propagation constant (β) is required for a maintained wave motion in both materials (ε_m for metal and ε_d for insulator). Therefore, the dispersion relation for SPPs at a single interface is

$$\beta = \frac{\omega}{c_0 \sqrt{\varepsilon_m \varepsilon_d / \varepsilon_m + \varepsilon_d}}. \quad (7)$$

With propagation constant (β), it is feasible to define the skin depths δ as $\delta = 1/2\gamma$ (Figure 4).

With a new term of surface plasmon frequency ($\omega_{\text{sp}} = \omega_p/\sqrt{1+\varepsilon_d}$) being defined, (7) leads to a dispersion plot for SPPs. For the air-metal case, the surface plasmon frequency is 0.707 ω_p.

In Figure 5, there is a bandgap between ω_{sp} and ω_p, when the curve only gives imaginary propagation constant (evanescent waves). When $\omega < \omega_{\text{sp}}$, SPP modes in TM polarization exist. A very large β value can be obtained at ω_{sp}, which denotes a point of resonance at that frequency point, namely the SP resonant oscillation. When $\omega > \omega_p$, $\varepsilon_m > 0$; so metal will exhibit dielectric behaviors with radiation unbounded to insulator since the mode lies above the lightline. The dispersion relation plotted above does not take damping factor into account, which will instead force a finite wave vector Re[β] at ω_{sp} due to the damping of free-electron oscillations. In this case, the right-hand side of (7) becomes a complex value and the dispersion will also slightly differ from the case of ideal conductors [16].

The single-interface case introduced above suggests several important characters related to SPPs. Firstly, a sustained surface wave can be excited along metal surfaces accompanied by ohmic loss, although at the same frequency bulk metal remains "opaque" for EM waves. Secondly, a bounded solution exists even with a half-space metal-cladded insulator, which means the SPP mode is confined to a single interface of metal-insulator with small out-of-plane radiation. Thirdly, the propagation constant of SPP mode is larger than that of a lightline at the same frequency point when the driving field has less-than-ω_{sp} frequency, which indicates a smaller effective wavelength for SPP mode compared to optical mode at same frequency. These three features are the sources of most applications reviewed in this article, and are the fundamentals of many prior efforts.

3.3. Metal-Insulator-Metal (MIM) Waveguides. Although surface plasmons can be confined to the metal-insulator boundary, the mode spread of the SP waves depends on the configuration of the waveguides and also the frequency. The length of the evanescent tail in a waveguide medium can

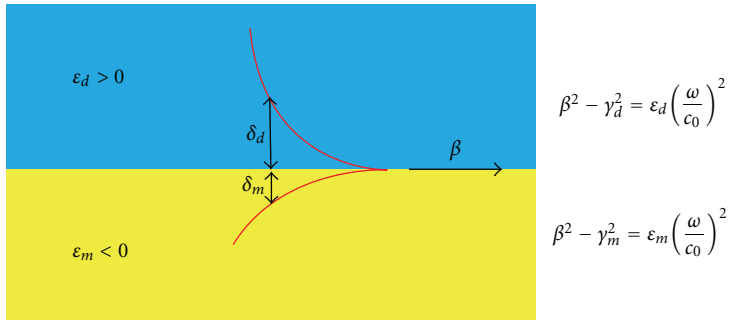

Figure 4: Definition of skin depths and their relation with propagation constant.

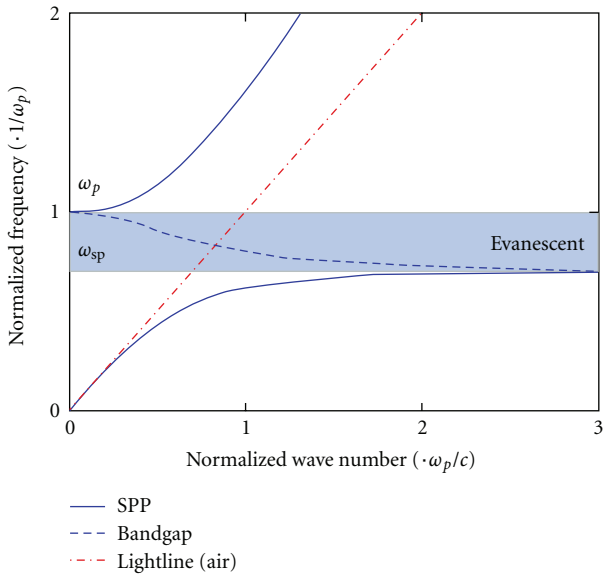

Figure 5: Dispersion relation of SPP (solid) in metal-insulator configuration. The curve for the frequency between 0.707 and 1 denotes imaginary propagation constant.

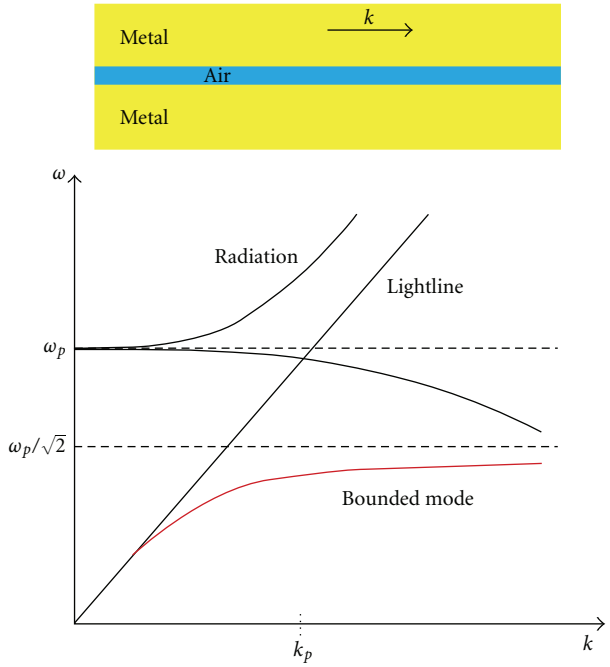

Figure 6: Dispersion plot for the MIM-layered structure adapted from [1].

be approximated by $\delta = 1/2\gamma$, when γ is defined from the conservation of momentum as follows:

$$\beta^2 - \gamma_d^2 = \varepsilon_d \left(\frac{\omega}{c_0}\right)^2 \quad (8)$$

$$\beta^2 - \gamma_m^2 = \varepsilon_m \left(\frac{\omega}{c_0}\right)^2. \quad (9)$$

Table 2 shows that for the metal-insulator (MI) waveguide, the evanescent tails can be very long compared to wavelength. For subwavelength and deep subwavelength mode confinement, it is necessary to explore different waveguide forms. The following section will start from an important plasmonic waveguide, namely metal-insulator-metal (MIM) waveguide.

The idea to incorporate surface plasmons to guided EM waves can be traced back to 1969, in Economou's paper [1] on theoretical study of EM field inside thin-films configuration. Note that it was about 30 years later, with the progress of advanced simulation tools and microscale fabrication technology, that people started to characterize plasmonic waveguides at optical frequencies.

A simple yet important form of plasmonic waveguide is based on a metal-insulator-metal (MIM) configuration (Figure 6). This waveguide, as its name indicates, consists of three layers with a dielectric core of either air or other insulator (usually with low optical loss and comparatively small refractive index), sandwiched by two metal claddings. In Economou's work [1], the dispersion relation for MIM configuration is analytically solved. In recent years, detailed analytical [17, 18] and experimental studies [19] of MIM are still performed and reported.

As verified by extensive numerical analysis, MIM waveguides possess notable tradeoff between acceptable propagation loss and subwavelength mode size. Veronis and Fan [20], along with Feigenbaum and Orenstein [21], have performed 3-dimensional (3D) simulation and mode analysis for MIM (sometimes called MDM for metal-dielectric-metal too)

Table 2: The lengths of evanescent tails at different wavelengths for metal-insulator boundary.

Wavelength (λ)	0.5 μm	1.55 μm	10.5 μm	300 μm
Frequency (c_0/λ)	600 THz	193 THz	28 THz	1 THz
ε_{Al}	$-36.5 + j9.4$	$-252 + j46$	$-8e3 + j5.2e3$	$-6e4 + j9e4$
ε_{Air}	1.0	1.0	1.0	1.0
Decay factor (γ/k_0)	0.1678	0.0631	0.0112	0.0041
Tail length (δ)	0.23 μm	1.95 μm	74.7 μm	5800 μm
Relative tail length (δ/λ)	0.47	1.26	7.12	19.49

Table 3: TM-mode size comparison for dielectric and plasmonic waveguides with λ = 1550 nm light. Data acquired from FDTD Solutions's integrated mode solver (http://www.lumerical.com/).

Waveguide type	Dielectric	MIM	IMI	MI
Materials	Silicon	Silver, air	Silver, air	Silver, air
Core thickness	300 nm	30 nm	30 nm	—
Total cladding thickness	—	300 nm	300 nm	—
n_{eff}	2.5060	1.5788	2.7104	1.0039
Loss (dB/cm)	—	2180.5	846.5	44.0
FWHM (H intensity)	208 nm	46 nm	148 nm	983 nm

structures. They successfully show that while the mode size of MIM can be pushed down to very close to the physical dimension of the guiding core in deep subwavelength regime, the acceptable propagation length keeps MIM waveguides competitive for on-chip signal transmission (Table 3). The 2D to 3D transition is verified by shrinking a 2D nanoslit [1] to a 3D nanospot [20, 22]. This feature brings in the possibility of using MIM structure as a device to guide propagating waves in ultrasmall dimension (Figure 7), and therefore an interesting platform for applications that require extreme field confinement or intensified light-matter interactions. The metal sandwich could possibly contain unwanted scattering loss from rough surfaces, which is another advantage of the MIM configuration.

From a transfer matrix perspective, it has been shown that if the fundamental TM mode is excited inside an MIM gap, the waveguide works well as a transmission line (TL) system, and shows reduced scattering loss from sharp bend [23], unlike traditional optical waveguides. The transmission line (TL) theory, adopted from the microwave realm, has then been applied to cascaded MIM systems [24] to study the reflection and transmission coefficient for complex or multilevel compositions of MIM waveguides. The formalism of TL theory based on eigenmode expansion, is found to be successful especially in calculating the coupling efficiency between SP waves propagated through several MIMs.

Along with the MIM waveguide, the insulator-metal-insulator (IMI) configuration has also found many applications. IMI is formed by burying a thin metal core in dielectric background, and if the symmetry condition is strictly met, a TM mode very similar to a dielectric mode can be supported. Devices incorporating IMI have been demonstrated for both passive [25] and active [26] cases, and because IMI's propagation loss is considerably smaller than MIM, it is frequently used for transmitting NIR optical power in longer distance above 10 μm's mark. The lack of mode confinement, however, hampers its usage in deep subwavelength scale, so does it with metal-insulator (MI) waveguides (Table 3).

Based on the MIM platform highlighted with extreme power confinement, several inventions or discoveries are noteworthy. Atwater and his coworkers have contributed significantly to this topic with their characterization of MIM plasmonic waveguides [27]. Chen [28] from Cornell University evaporated gold onto silicon ribs to form MIM waveguide, which also developed a novel way to effectively excite SP modes from photons. On the field of active plasmonics, nanocavities formed in MIM waveguide are proposed for fast modulation [29, 30], and have exhibited great potentials for development of future small-print modulators.

It is also interesting to look at the MIM waveguide from a different perspective. If an MIM waveguide is chopped for a very small propagation (less than one hundred nanometers, e.g.,), and at the same time a light beam illuminates right into the waveguide from free space, the situation will be very close to transmission through an optical head [31], which can be used to count the power getting through a subwavelength slit or a hole inscribed on a thin film. One important literature published on extra transmission related to SP waves is from Ebbesen et al. [9]. In this paper, the observance of at least 10-folds of transmission enhancement is reported (Figure 8), after facilitated features of surface corrugations are applied. Ironically, such an important literature later is cited by the authors themselves that the reported enhancement is greatly exaggerated because of a problematic measurement. The role of plasmonics in extra transmission is therefore under debate, as [32] and especially [33] have reviewed. One of the authors from the original nature paper, Tineke Thio, converted to be one of the most radical opponents to the role of surface plasmons in enhanced transmission. A diffraction theory [32], from her point of view, is powerful enough to explain most phenomena observed in extratransmission.

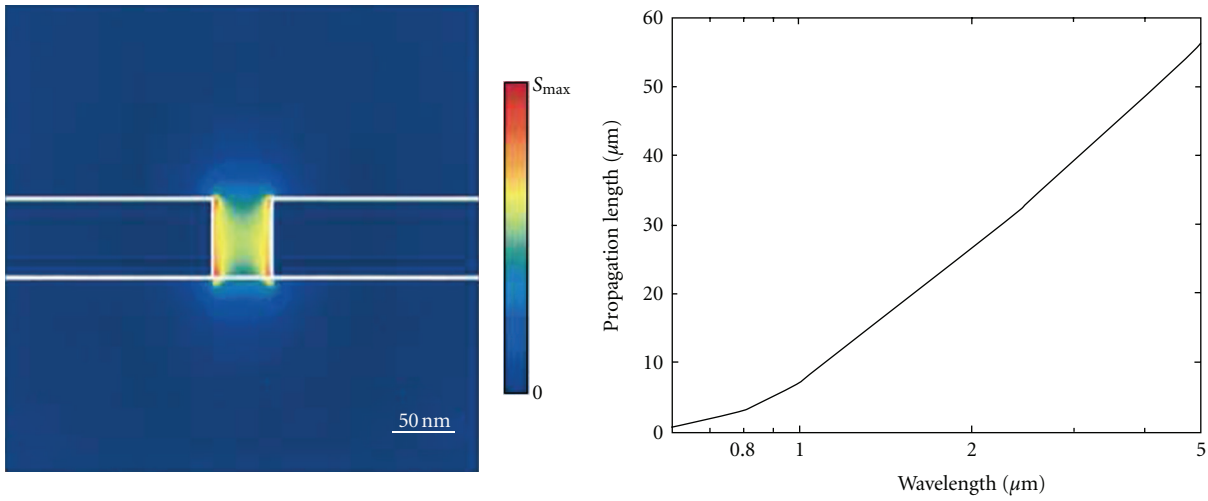

Figure 7: (a) A typical MIM-mode profile for 1550 nm light inside a 50 nm-by-50 nm air gap. The substrate and superstrate are silicon dioxide and air, respectively. (b) Propagation distance of the MIM mode for optical to NIR frequency [20].

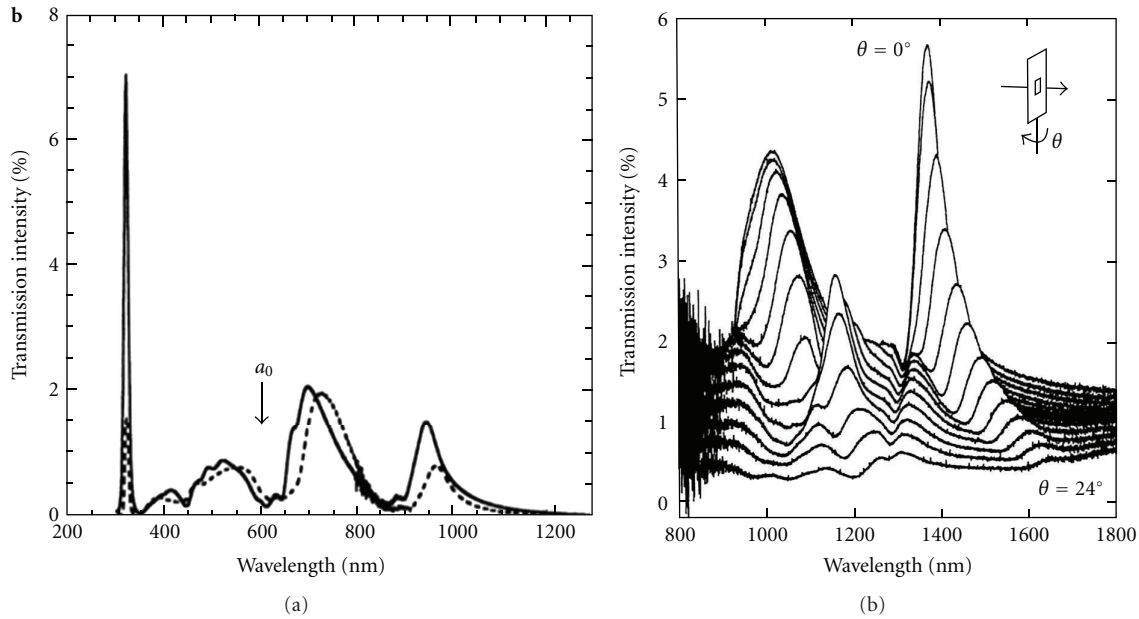

Figure 8: Transmission through subwavelength holes patterned in Ag as a function of wavelength (a) and illumination angle (b) [9].

Despite all the debates, it is then impossible to halt the eagerness of researchers on utilizing SP waves to accomplish higher transmission through subwavelength holes or slits. For example, Pacifici et al. [34] have used a near-field detector to characterize the field profile when corrugated surfaces are illuminated by plane waves. They managed to observe subwavelength focusing of light and have given their own physical model to explain it. A carefully designed mask [35] is found to be able to achieve a subwavelength transmission *beyond* near-field with radiationless interference. This discovery might be more interesting than the previous one for far-field applications such as imaging and nanolithography. More and more theoretical calculations on EM waves among periodic surface features or slit diffraction such as [36, 37] or [38] are still being elaborated and published, providing fresh approaches or understandings into this topic.

The extratransmission experiments introduced above are mostly based on incident plane waves from free space or uniform dielectric half space. In 2007, Veronis and Fan published simulation results [39] studying the behavior of NIR light when a dielectric waveguide is butt-connected to an MIM waveguide. They find that although the mode profiles between dielectric and MIM waveguides differ greatly, a transmission of ~70% can be achieved. There are

quite a few previous unknowns mentioned by this theoretical analysis. Firstly, the mode overlap is not found as a key issue for coupling, as the "funneling" effect has been verified by numerical simulation performed recently [40]. Secondly, the direct coupling only works for TM polarization, which is different compared to the classical case of an aperture antenna loaded on an infinite ground plane [41]. Therefore, a different physics unlike the aperture antenna theory must exist. Thirdly, the way that optical modes couple to SP modes are different to TL formalism. A matched propagation constant here does not necessarily guarantee an optimal coupling efficiency, as the eigenmodes in plasmonic waveguides are different in nature regarding the orthonormality compared to conventional rectangular waveguides. As all being said, direct coupling remains an interesting topic to the plasmonics community and has always been appreciated as a practical scheme with plasmonic devices.

3.4. Subwavelength Waveguiding by Periodic Structures. Surface plasmons are grouped oscillations of free electrons near the surface. The coupling of plasmons and photons could happen on the boundary between a metal and an insulator. As the "donor" of plasmons, metals are usually designed to share a flat boundary with insulators to avoid unwanted out-of-plane scattering. Rough boundaries or surface corrugations, on the other hand, are occasionally introduced [16] for excitations or observations of SPPs. Theoretically, surface plasmons exist for middle infrared (MIR) or even far infrared (FIR) regime. We can recall the lengths of evanescent tails in the dielectric side are given by $1/2\gamma_d$, while the term γ_d is given by

$$\gamma_d = \sqrt{\beta^2 - \varepsilon_d \left(\frac{\omega}{c}\right)^2}. \tag{10}$$

For EM waves with frequencies much smaller than optical spectrum, ε_m is a negative term with large absolute value, thus the value of γ_d can be very small. For a metal-insulator case with $|\varepsilon_m| \gg |\varepsilon_d|$, and referring to the dispersion relation in (7), we can see β^2 will approach $\varepsilon_d(\omega/c)^2$, which is the right side of (8). Therefore, γ_d will likely be very small and leads to a very long evanescent tail. This type of surface wave looks close to the so-called Zenneck or Sommerfeld wave [42] and the field confinement will be very poor (Table 3).

Obviously, to achieve tightly bounded surface wave beyond optical spectrum such as terahertz (THz) or even gigahertz (GHz) regime, a flat surface is not enough. On the other hand, the lower frequency (or the longer wavelength) makes it possible to make comparatively small corrugation on metallic surfaces. If the considered corrugation is small enough compared to wavelength, it can be legitimately characterized by using the effective medium formalism. This approach is called "spoof plasmonics" by Pendry et al. [43], in their attempt to achieve arbitrary "spoof" plasma frequency via drilling holes on the perfect electric conductor (PEC).

When the corrugation is uniformly distributed in xy direction (Figure 9(a)), the bulk PEC can be regarded as a uniaxial crystal, a typical anisotropic metamaterial. The dispersion calculation yields an upper cutoff frequency and an extremely slow light towards this cut-off, same as the typical SPP behaves. More importantly, when an effective medium is used for analysis, the theory of conventional plasmonics can be applied to the structured surface. Therefore, the concept of surface plasmon frequency can also be extended to describe the property of this metamaterial. Instead of the canonical value, the new (or effective) surface plasmon frequency is determined by the dimension of surface corrugations. Therefore, the optical property of this metamaterial can be well controlled by tweaking the physical perturbations applied to the bulk material.

The spoof plasmonic approach has inspired many discoveries based on surface corrugations especially in THz region as metals are almost lossless and compact THz waveguides are in high demand. Maier et al. [44] designs a THz waveguide for subwavelength confinement in 2D working at 1 THz. Martin-Cano et al. have designed metal gratings as THz waveguide platform, which can integrate multiple passive devices at the same time [45]. In GHz region, Zhao et al. [46] used designer surface plasmon approach to demonstrate the same concept (Figure 10).

Another platform for spoof plasmonics is based on stratified medium, which finds vast applications in the optical regime. Multilayered composites with periodic layer-unit have been widely implored as negative index materials (NIMs) for superlensing. Treated as an effective medium, its anisotropy is well approximated by straightforward mixing rules [47, 48] if each repeated layer is thin enough compared to wavelength. Along with the superlensing effect [49], multilayered composites have also been designed to support surface-plasmon-like waves [50, 51] and used for nanolithography. Figure 11 shows the schematic electric field diagram of a multilayer structure, when a composition of surface waves is formed [48].

4. Plasmonic Materials and Fabrication Technique

The progress of experimental plasmonics is closely related to the advancement of material research and fabrication technology. Plasmonic phenomena have been observed and investigated for more than 40 years, originally on light scattering from metal particles in early years, gradually including light guiding by particle arrays and layered structures. Without the advanced fabrication methods to process plasmonic materials and integrate plasmonic structures into optical circuitry, it is impossible to expect the vast applications of plasmonic components in sensing, imaging, storage, and communications these days. In this section, the most important plasmonic materials and their processing methods will be reviewed.

In solid-state physics, surface plasmons are treated as grouped oscillation of electron gas. The electron gas model fits materials with a high volume of free electrons, which is inherently more accurate for simple metals (alkali metals). Metals found in semiconductor technology at room temperature have an electron concentration close to the order

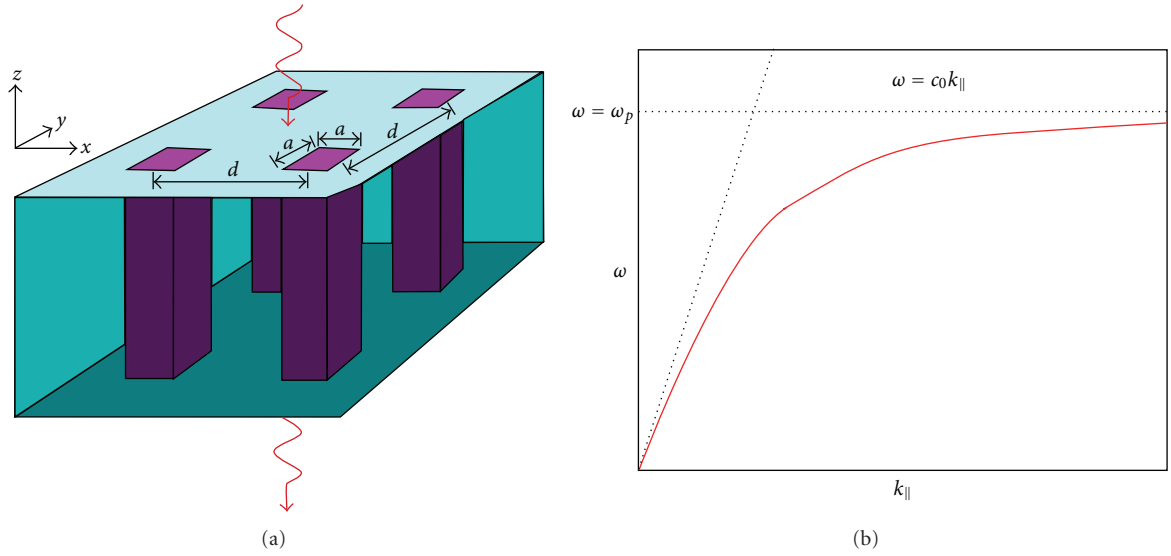

Figure 9: Spoof plasmonics in PEC shown by dimension (a) and dispersion (b) [43].

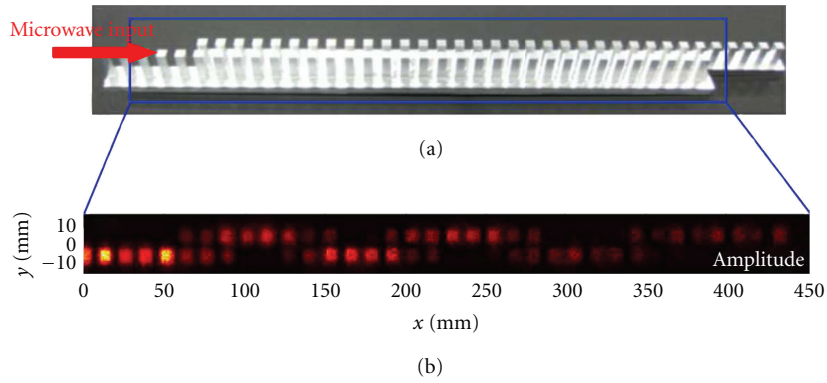

Figure 10: A spoof plasmonic waveguide guiding GHz waves [46], forming a directional coupler.

of 10^{22} per cm^3, while semiconductors or doped materials widely used in this industry have a carrier concentration of less than 10^{17} per cm^3. As a result, most plasmonic structures, especially those for optical spectrum, will involve metals at some level. The overwhelmingly used materials in plasmonics have remained to be those that are stable in room temperature, especially aluminum (Al) and noble metals such as gold (Au), silver (Ag), and copper (Cu) (Table 1). Alternative plasmonic materials known to contain abundant free carriers include metallic alloys, metallic compounds, and graphene.

4.1. Metals. Metals have been studied and understood through the free-electron model, in which the electrons inside metals are regarded as moving almost free from striking with each other. In the Drude formalism for 3D electron gas, the mean relaxation time is described by the damping frequency term γ_τ. For the noble metals frequently used in plasmonics, the total damping comes from not only the interactions between conduction electrons, but also from interband transitions [10, 16]. Wherever the damping of free-electron oscillation actually comes from, the propagation loss in classical electromagnetic problems for plasmonic metals can be evaluated from the imaginary parts of their dielectric constants and the electric field intensity, treated as dissipated or lost in the form of ohmic heat. Therefore, a straightforward figure of merit for choosing plasmonic material is its resistivity. By reading the optical resistivity data or the dielectric constants of various metals [52], it is possible to spot candidates of suitable materials for different frequency ranges. In NIR spectrum, silver has the smallest imaginary part of permittivity and the best conductivity, making it a highly favored material. The easy oxidation somehow limits its applications, and makes gold a popular candidate in this frequency range. For the applications of UV or DUV light such as the 193 nm light for DUV optical lithography, however, aluminum is proved to be the most attractive candidate [12] (Table 1).

Processing metals (especially noble metals) is in general complex, especially compared with semiconductors used in microfabrication. The deposition of plasmonic metals can be achieved in vacuum by sputtering or evaporation. To avoid percolation, and to obtain acceptable uniformity and quality,

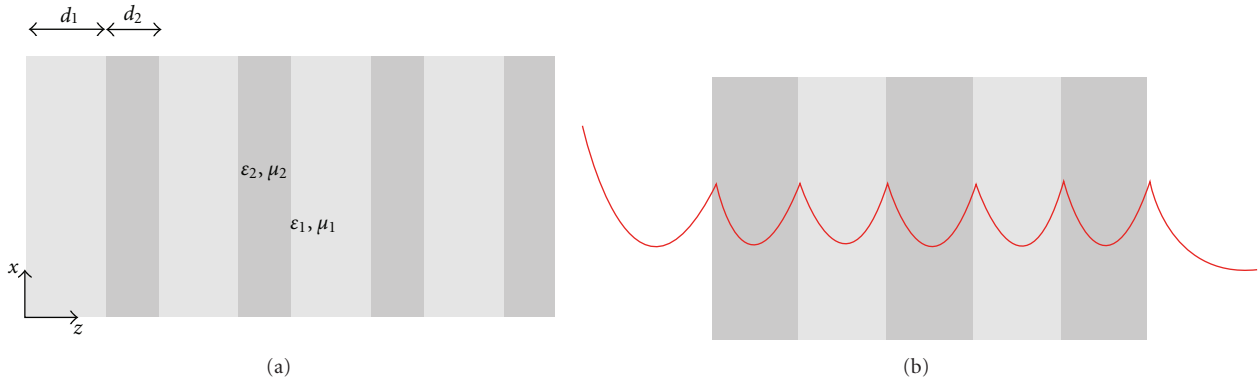

Figure 11: Multilayered, periodic metal-insulator stacks (a) and the schematic *E*-field profile (b) inside [48].

the deposition rate is usually limited to less than 1 nm per second. The small deposition rate is normally not a big issue as in most cases the required thickness for plasmonics is small. Electroplating gives faster metal growth rate but the quality of the surface might not be considered fine enough for plasmon waves.

The pattern transfer from resist to metals is extremely challenging for noble metals, as there are not many effective methods to etch copper, silver, or gold. Plasmonic metals such as aluminum can be etched by plasma etch in Cl_2-based ambient. Other than this, there are generally two approaches to pattern metals. The first one is through image reversal and lift-off process, which requires resist overhang after development. There have been photoresists specifically used for lift-off process such as nLOR from MicroChem [53], while researchers also use bilayer or multilayer compositions to achieve the crucial overhang [54]. When using bilayer resists for liftoff, it is conventionally required to coat a bottom resist layer for at least twice as thick as the lift-off thickness. Therefore, it is not easy to have high aspect ratio, standalone metal features fabricated. A second approach to pattern metal is through ion milling. Focused ion beam can be used to directly mill patterns into gold or silver film, while it usually introduces redepositions from the beam source. Argon ion beam is another option that can work with noble metals, which requires hard masks such as carbon and might greatly increase the number of steps and also the complexity of processing.

4.2. Compounds. Metal silicides are originally used to decrease the contact resistivity in VLSI circuits and especially MOSFET technology. As they have an intermediate conductivity and carrier concentration between metal and semiconductor, silicide compounds have also been investigated for plasmonic applications especially in THz frequency [55]. In the form of compounds consisting of silicon and metals (Ti, Co, W, Ni, Pd, etc.), silicides have a smaller plasmonic frequency compared to noble metals used in the near-infrared regime and in general higher loss. However, as its fabrication and electric property have been extensively studied for large-scale integrated circuit technology, the deposition of very thin layers and accurate patterning is highly reliable.

Transparent conducting oxide (TCO) materials are optically transparent and electrically conductive. As one of the most widely used TCO, Indium tin oxide (ITO) has been widely studied and used in display industry and optoelectronics as an optical coating. The frequency range for ITO to exhibit negative permittivity is also in NIR, in which ITO is reported to have competitively low loss even compared to silver. The deposition of ITO films can be achieved through sputter deposition [56]. The major concern about using ITO is its price, and the instability of its optical property for different growth conditions. Similar materials include aluminum zinc oxide (AZO), gallium zinc oxide (GZO), and so forth [57].

4.3. Graphene and Others. A few rarely-used yet interesting materials exist as potential candidates for plasmonic applications. Among them, graphene and polymer-based plasmonics have attracted more and more attention, because of the distinguished electronic and optical properties. Graphene's plasmonic property has been predicted in [58–60], showing promising tunable optical conductivity. Standard approaches for graphene layer deposition are limited at this time, although depositions based on transfer-printing method [61], CVD [62], and electrostatic method [63] have been reported.

5. Conclusion

Surface plasmon has been studied extensively for optical sensing and imaging, even long before the term "plasmonics" became widely accepted. The transition from SPR in standalone devices to plasmonics, assisted by advanced simulation and fabrication tools, emphasizes the integration of plasmonic features into subsystems for all sorts of optical communications and information exchange. With more and more significant discoveries based on surface plasmon waveguiding in subwavelength or deep subwavelength regime, plasmonics is expected to further impact the research and development of integrated optical communications, data storage, optical sensing, and imaging technology.

Acknowledgment

This paper is based upon work supported in part by the U. S. Army under Award no. W911NF-10-1-0153 and the National Science Foundation under Award no. ECCS-1057381. Acknowledgment is made to the Donors of the American Chemical Society Petroleum Research Fund for partial support of this project.

References

[1] E. N. Economou, "Surface plasmons in thin films," *Physical Review*, vol. 182, no. 2, pp. 539–554, 1969.

[2] R. H. Ritchie, "Surface plasmons in solids," *Surface Science*, vol. 34, no. 1, pp. 1–19, 1973.

[3] M. I. Stockman, "Nanoplasmonics: past, present, and glimpse into future," *Optics Express*, vol. 19, no. 22, pp. 22029–22106, 2011.

[4] K. S. Kim, "On the evolution of PON-based FTTH solutions," *Information Sciences*, vol. 149, no. 1–3, pp. 21–30, 2003.

[5] M. Rothschild, "A roadmap for optical lithography," *Optics and Photonics News*, vol. 21, no. 6, pp. 26–31, 2010.

[6] J. Eid, A. Fehr, J. Gray et al., "Real-time DNA sequencing from single polymerase molecules," *Science*, vol. 323, no. 5910, pp. 133–138, 2009.

[7] W. A. Challener, C. Peng, A. V. Itagi et al., "Heat-assisted magnetic recording by a near-field transducer with efficient optical energy transfer," *Nature Photonics*, vol. 3, no. 4, pp. 220–224, 2009.

[8] M. L. Brongersma and P. G. Kik, *Surface Plasmon Nanophotonics*, Springer, Dordrecht, The Netherlands, 2007.

[9] T. W. Ebbesen, H. J. Lezec, H. F. Ghaemi, T. Thio, and P. A. Wolff, "Extraordinary optical transmission through subwavelenght hole arrays," *Nature*, vol. 391, no. 6668, pp. 667–669, 1998.

[10] C. Kittel, *Introduction to Solid State Physics*, John Wiley & Sons, New York, NY, USA, 1989.

[11] B. E. A. Salen and M. C. Teich, *Fundamentals of Photonics*, Wiley-Interscience, Hoboken, NJ, USA, 2nd edition, 2007.

[12] M. A. Ordal, R. J. Bell, J. Alexander, L. L. Long, and M. R. Querry, "Optical properties of fourteen metals in the infrared and far infrared: Al, Co, Cu, Au, Fe, Pb, Mo, Ni, Pd, Pt, Ag, Ti, V, and W," *Applied Optics*, vol. 24, no. 24, pp. 4493–4499, 1985.

[13] E. D. Palik, *Handbook of Optical Constants of Solids*, Academic Press, Orlando, Fla, USA, 1985.

[14] J. D. Joannopoulos, S. G. Johnson, and J. N. Winn, *Photonic Crystals: Molding the Flow of Light*, Princeton University Press, New Jersey, NJ, USA, 2008.

[15] N. Engheta and R. W. Ziolkowski, *Metamaterials: Physics and Engineering Explorations*, Wiley, 2006.

[16] S. A. Maier, *Plasmonics: Fundamentals and Applications*, Springer, New York, NY, USA, 2007.

[17] R. Gordon, "Light in a subwavelength slit in a metal: propagation and reflection," *Physical Review B*, vol. 73, no. 15, Article ID 153405, 2006.

[18] J. A. Dionne, L. A. Sweatlock, H. A. Atwater, and A. Polman, "Plasmon slot waveguides: towards chip-scale propagation with subwavelength-scale localization," *Physical Review B*, vol. 73, no. 3, Article ID 035407, 9 pages, 2006.

[19] S. I. Bozhevolnyi, V. S. Volkov, E. Devaux, J.-Y. Laluet, and T. W. Ebbesen, "Channel plasmon subwavelength waveguide components including interferometers and ring resonators," *Nature*, vol. 440, no. 7083, pp. 508–511, 2006.

[20] G. Veronis and S. Fan, "Guided subwavelength plasmonic mode supported by a slot in a thin metal film," *Optics Letters*, vol. 30, no. 24, pp. 3359–3361, 2005.

[21] E. Feigenbaum and M. Orenstein, "Modeling of complementary (Void) plasmon waveguiding," *Journal of Lightwave Technology*, vol. 25, no. 9, pp. 2547–2562, 2007.

[22] R. Yang, M. A. G. Abushagur, and Z. Lu, "Efficiently squeezing near infrared light into a 21nm-by-24nm nanospot," *Optics Express*, vol. 16, no. 24, pp. 20142–20148, 2008.

[23] G. Veronis and S. Fan, "Bends and splitters in metal-dielectric-metal subwavelength plasmonic waveguides," *Applied Physics Letters*, vol. 87, no. 13, Article ID 131102, 3 pages, 2005.

[24] Ş. E. Kocabaş, G. Veronis, D. A. B. Miller, and S. Fan, "Modal analysis and coupling in metal-insulator-metal waveguides," *Physical Review B*, vol. 79, no. 3, Article ID 035120, 2009.

[25] R. Charbonneau, C. Scales, I. Breukelaar et al., "Passive integrated optics elements based on long-range surface plasmon polaritons," *Journal of Lightwave Technology*, vol. 24, no. 1, pp. 477–494, 2006.

[26] T. Nikolajsen, K. Leosson, and S. I. Bozhevolnyi, "Surface plasmon polariton based modulators and switches operating at telecom wavelengths," *Applied Physics Letters*, vol. 85, no. 24, pp. 5833–5835, 2004.

[27] J. A. Dionne, H. J. Lezec, and H. A. Atwater, "Highly confined photon transport in subwavelength metallic slot waveguides," *Nano Letters*, vol. 6, no. 9, pp. 1928–1932, 2006.

[28] L. Chen, J. Shakya, and M. Lipson, "Subwavelength confinement in an integrated metal slot waveguide on silicon," *Optics Letters*, vol. 31, no. 14, pp. 2133–2135, 2006.

[29] J. A. Dionne, K. Diest, L. A. Sweatlock, and H. A. Atwater, "PlasMOStor: a metal-oxide-si field effect plasmonic modulator," *Nano Letters*, vol. 9, no. 2, pp. 897–902, 2009.

[30] W. Cai, J. S. White, and M. L. Brongersma, "Compact, high-speed and power-efficient electrooptic plasmonic modulators," *Nano Letters*, vol. 9, no. 12, pp. 4403–4411, 2009.

[31] M. J. Levene, J. Korlach, S. W. Turner, M. Foquet, H. G. Craighead, and W. W. Webb, "Zero-mode waveguides for single-molecule analysis at high concentrations," *Science*, vol. 299, no. 5607, pp. 682–686, 2003.

[32] H. J. Lezec and T. Thio, "Diffracted evanescent wave model for enhanced and suppressed optical transmission through subwavelength hole arrays," *Optics Express*, vol. 12, no. 16, pp. 3629–3651, 2004.

[33] T. Thio, "A bright future for subwavelength light sources," *American Scientist*, vol. 94, no. 1, p. 40, 2006.

[34] D. Pacifici, H. J. Lezec, L. A. Sweatlock, R. J. Walters, and H. A. Atwater, "Universal optical transmission features in periodic and quasiperiodic hole arrays," *Optics Express*, vol. 16, no. 12, pp. 9222–9238, 2008.

[35] R. Merlin, "Radiationless electromagnetic interference: evanescent-field lenses and perfect focusing," *Science*, vol. 317, no. 5840, pp. 927–929, 2007.

[36] F. J. García-Vidal, S. G. Rodrigo, and L. Martín-Moreno, "Foundations of the composite diffracted evanescent wave model," *Nature Physics*, vol. 2, no. 790, pp. 262–267, 2006.

[37] L. Chen, J. T. Robinson, and M. Lipson, "Role of radiation and surface plasmon polaritons in the optical interactions between a nano-slit and a nano-groove on a metal surface," *Optics Express*, vol. 14, no. 26, pp. 12629–12636, 2006.

[38] D. Pacifici, H. J. Lezec, H. A. Atwater, and J. Weiner, "Quantitative determination of optical transmission through subwavelength slit arrays in Ag films: role of surface wave interference

and local coupling between adjacent slits," *Physical Review B*, vol. 77, no. 11, Article ID 115411, 2008.

[39] G. Veronis and S. Fan, "Theoretical investigation of compact couplers between dielectric slab waveguides and two-dimensional metal-dielectric-metal plasmonic waveguides," *Optics Express*, vol. 15, no. 3, pp. 1211–1221, 2007.

[40] R. A. Wahsheh, Z. Lu, and M. A. G. Abushagur, "Nanoplasmonic couplers and splitters," *Optics Express*, vol. 17, no. 21, pp. 19033–19040, 2009.

[41] C. A. Balanis, *Antenna Theory: Analysis and Design*, Wiley, New Jersey, NJ, USA, 2005.

[42] A. Sommerfeld, "Propagation of waves in wireless telegraphy," *Annals of Physics*, vol. 81, pp. 1367–1153, 1926.

[43] J. B. Pendry, L. Martín-Moreno, and F. J. Garcia-Vidal, "Mimicking surface plasmons with structured surfaces," *Science*, vol. 305, no. 5685, pp. 847–848, 2004.

[44] S. A. Maier, S. R. Andrews, L. Martín-Moreno, and F. J. García-Vidal, "Terahertz surface plasmon-polariton propagation and focusing on periodically corrugated metal wires," *Physical Review Letters*, vol. 97, no. 17, Article ID 176805, 4 pages, 2006.

[45] D. Martin-Cano, M. L. Nesterov, A. I. Fernandez-Dominguez, F. J. Garcia-Vidal, L. Martin-Moreno, and E. Moreno, "Domino plasmons for subwavelength terahertz circuitry," *Optics Express*, vol. 18, no. 2, pp. 754–764, 2010.

[46] W. Zhao, O. M. Eldaiki, R. Yang, and Z. Lu, "Deep subwavelength waveguiding and focusing based on designer surface plasmons," *Optics Express*, vol. 18, no. 20, pp. 21498–21503, 2010.

[47] D. J. Bergman, "The dielectric constant of a composite material-a problem in classical physics," *Physics Reports*, vol. 43, no. 9, pp. 377–407, 1978.

[48] B. Wood, J. B. Pendry, and D. P. Tsai, "Directed subwavelength imaging using a layered metal-dielectric system," *Physical Review B*, vol. 74, no. 11, Article ID 115116, 2006.

[49] W. Cai, D. A. Genov, and V. M. Shalaev, "Superlens based on metal-dielectric composites," *Physical Review B*, vol. 72, no. 19, Article ID 193101, 4 pages, 2005.

[50] J. Elser, A. A. Govyadinov, I. Avrutsky, I. Salakhutdinov, and V. A. Podolskiy, "Plasmonic nanolayer composites: coupled plasmon polaritons, effective-medium response, and subdiffraction light manipulation," *Journal of Nanomaterials*, vol. 2007, Article ID 79469, 8 pages, 2007.

[51] R. Yang, X. Huang, and Z. Lu, "Arbitrary super surface modes bounded by multilayered metametal," *Micromachines*, vol. 3, no. 1, pp. 45–54, 2012.

[52] D. R. Lide, *CRC Handbook of Chemistry and Physics*, CRC Press, 2004.

[53] MicroChem Corp, March2012, http://www.microchem.com.

[54] Photolithography Resist Processes and Capabilities (CNF), March 2012, http://www.cnf.cornell.edu/cnf_process_photo_resists.html.

[55] R. A. Soref, S.-Y. Cho, W. Buchwald, and R. E. Peale, "Silicon plasmonic waveguides," in *Silicon Photonics for Telecommunications and Biomedical Applications*, B. Jalali and S. Fathpour, Eds., Taylor & Francis, London, UK, 2010.

[56] "PVD 75 Sputter Deposition from Kurt J. Lesker by CNF," March 2012, http://www.cnf.cornell.edu/cnf5_tool.taf?_function=detail&eq_id=156.

[57] P. R. West, S. Ishii, G. V. Naik, N. K. Emani, V. M. Shalaev, and A. Boltasseva, "Searching for better plasmonic materials," *Laser & Photonics Reviews*, vol. 4, no. 6, pp. 795–808, 2010.

[58] D. R. Andersen, "Graphene-based long-wave infrared TM surface plasmon modulator," *Journal of the Optical Society of America B*, vol. 27, no. 4, pp. 818–823, 2010.

[59] F. H. L. Koppens, D. E. Chang, and F. J. Garciía de Abajo, "Graphene plasmonics: a platform for strong Light-Matter interactions," *Nano Letters*, vol. 11, no. 8, pp. 3370–3377, 2011.

[60] J. T. Kim and S.-Y. Choi, "Graphene-based plasmonic waveguides for photonic integrated circuits," *Optics Express*, vol. 19, no. 24, pp. 24557–24562, 2011.

[61] X. Li, Y. Zhu, W. Cai et al., "Transfer of large-area graphene films for high-performance transparent conductive electrodes," *Nano Letters*, vol. 9, no. 12, pp. 4359–4363, 2009.

[62] A. Reina, X. Jia, J. Ho et al., "Large area, few-layer graphene films on arbitrary substrates by chemical vapor deposition," *Nano Letters*, vol. 9, no. 1, pp. 30–35, 2009.

[63] A. N. Sidorov, M. M. Yazdanpanah, R. Jalilian, P. J. Ouseph, R. W. Cohn, and G. U. Sumanasekera, "Electrostatic deposition of graphene," *Nanotechnology*, vol. 18, no. 13, Article ID 135301, 2007.